Ultrafast structural color change in indium tin oxide/titanium dioxide 1D photonic crystal

Liliana Moscardi [1,2], Stefano Varas [3], Alessandro Chiasera [3], Francesco Scotognella [1,2], Michele Guizzardi [1]

[1] *Dipartimento di Fisica, Politecnico di Milano, Piazza Leonardo da Vinci 32, 20133 Milano, Italy*

[2] *Center for Nano Science and Technology@PoliMi, Istituto Italiano di Tecnologia (IIT), Via Giovanni Pascoli, 70/3, 20133, Milan, Italy*

[3] *Istituto di Fotonica e Nanotecnologie IFN – CNR, Via alla Cascata, 56/C, 3812, Povo – Trento, Italy*

Abstract

Photonic crystals can integrate plasmonic materials such as indium tin oxide in their structure. Exploiting indium tin oxide plasmonic properties, it is possible to tune the photonic band gap of the photonic crystal upon the application of an external stimuli. In this work, we have fabricated a one-dimensional multilayer photonic crystal via radiofrequency sputtering and we have triggered its optical response with ultrafast pump-probe spectroscopy. Upon photoexcitation, we observe a change in the refractive index of indium tin oxide. Such an effect has been used to create a photonic crystal that change its photonic bandgap in an ultrafast time scale. All optical modulation in the visible region, that can be tuned by designing the photonic crystal, has been demonstrated.

Keywords: indium tin oxide; ultrafast spectroscopy; photonic crystal

Introduction:

Photonic crystals (PCs) represent a class of periodic structures that can be integrated into a wide range of technologies. Thanks to their high symmetry (in one, two or three dimensions) and the difference in terms of refractive indices of the constituent materials, an interference of the incident and diffused electromagnetic wave is generated, causing the formation of a forbidden band for the passage of photons, called photonic band gap (PBG) [1–4]. This attributes to PCs their peculiar optical properties and the generation of their changing colors, called structural colors. There are several applications in which multilayer PCs can be exploited, such as distributed feedback lasers [5–8], perfect absorbers [9,10], and sensors [11–15]. Selecting responsive materials for their fabrication, it is possible to modulate their optical response upon application of external stimuli. PCs can be fabricated with several techniques in one dimension, two dimensions and three dimensions [16]. Moreover, quasicrystals [17] and disordered structures [18,19] can be fabricated.

Multilayer PCs, also called Distributed Bragg Reflectors (DBRs), that include indium tin oxide are promising devices since this plasmonic material is able to show a high refractive index change with an applied electric field [20]. ITO-based DBRs take advantage of the ability to change their refractive index through the application of an electric field in order to modulate the position of the PBG. The optical properties of the multilayer can be easily tuned by acting on the refractive index of the constituent materials or on the geometric parameters of the lattice. [21,22].

In this work we have fabricated a one dimensional PC made by indium tin oxide and titanium dioxide via radiofrequency sputtering. The fabricated multilayer PC shows a very high optical quality with a strong PBG. By pumping the PC at 1550 nm, in the range of the plasma frequency of ITO, we observe in transient differential transmission measurements relaxation dynamics within the first picosecond of time delay. Such dynamics is mainly due to electron-phonon scattering in ITO. The ultrafast modulation of the plasma frequency of ITO results in an ultrafast modulation of the PBG of the ITO-based PC.

Experimental methods

Sample preparation: The multilayer ITO/TiO_2 structures were deposited on vitreous silica glass (v-SiO_2) by RF magnetron sputtering. The v-SiO_2 substrates have dimensions 75 mm × 25 mm × 1 mm. Before deposition, the substrates were ultrasonically cleaned in deionized water then they were cleaned with ethanol and finally dried in nitrogen. The substrates were after cleaned inside of the RF sputtering chamber for 10 min just before starting the deposition while heating up the temperature to 120 °C at a pressure of 10^{-6} mbar.

The magnetron RF sputtering deposition of ITO and TIO_2 films was performed by alternatively changing a 15 cm × 5 cm ITO and 15 cm × 5 cm TiO_2 targets. The residual pressure before the deposition was 4.5×10^{-7} mbar. During the deposition procedure, the substrates were not heated, and the sample holder temperature was kept at 30 °C. The sputtering was performed in an Ar atmosphere (5.4×10^{-3} mbar) and an RF power of 110 W was applied on TiO_2 target and 80 W applied on the ITO target. To monitor the thickness of the layers during the deposition, two quartz microbalances INFICON model SQM-160, faced on the two targets were employed. The final resolution on the effective thickness obtained by these quartz microbalances is about 1 Å. More details are available in reference [19]. The deposited structure consists of 5 couple ITO/TiO_2 for a total of 10 layers. The first layer deposited directly on the substrates is ITO while the last layer is TiO_2. Reference ITO and TIO_2 single layer were also fabricated using the same deposition protocol on silicon and vitreous silica glass substrates.

Optical characterization: The steady-state light transmission spectrum of the PC has been acquired with a JASCO spectrophotometer. The ultrafast differential transmission measurements have been performed by using a Coherent Libra amplified laser system with the fundamental wavelength at 800 nm, a pulse duration of about 100 fs and a repetition rate of 1 kHz. Noncollinear optical parametric amplifiers to tune the pump wavelength has been built with a procedure reported in Reference [23] with a fluence of 300uJ/cm^2. White light generation for the probe pulse has been achieved focusing the fundamental beam into a sapphire plate. The differential transmission $\Delta T/T = (T_{ON} - T_{OFF})/T_{OFF}$ has been acquired with an optical multichannel analyzer. T_{ON} and T_{OFF} indicate the probe spectra transmitted the excited and unperturbed sample, respectively.

Results and Discussion

In Figure 1 we can see the transmission of the ITO layer, which is transparent in the visible and we see decrease of transmittivity below 400 nm due to intragap state [24] and the more evident decrease where we have the band gap transition around 340 nm. Titanium dioxide is completely transparent in the visible and have a bandgap around 330 nm [25]. Thus, the interband absorption feature of titanium is significantly overlapped with glass adsorption, mainly to due to silicon dioxide interband absorption, as depicted in Figure 1a. As we discussed above the stacking of two dielectric materials (ITO and TiO_2) creates a PBG that completely changes the transmission compared to the one of the single layers, we can see the appearance of some dip where the transmission of the photon inside the structure is neglected. To estimate the thickness of the layers we have performed a fit of the experimental data with the transfer matrix method [26]. In the Supporting Information we report the fit of the transmission spectrum (Figure S1). For TiO_2 we have used the refractive index dispersion reported in Ref. [27]. For ITO, we have used a Drude model with parameters taken from Ref. [28] (i.e., $\varepsilon_\infty = 4$, $N = 2.49 \times 10^{26}\ charge/m^3$, $\Gamma = 0.1132\ eV$, that are, respectively, the high frequency dielectric constant, the number of carriers, the carrier damping). The contribution of ITO to the transmission spectrum is reported in Figures S2 and S3. The extracted thickness of the ITO layers is 100 nm and the extracted thickness of the TiO_2 layers is 79 nm. The PC is made of 5 bilayers. Thus, the total thickness of the PC is 895 nm.

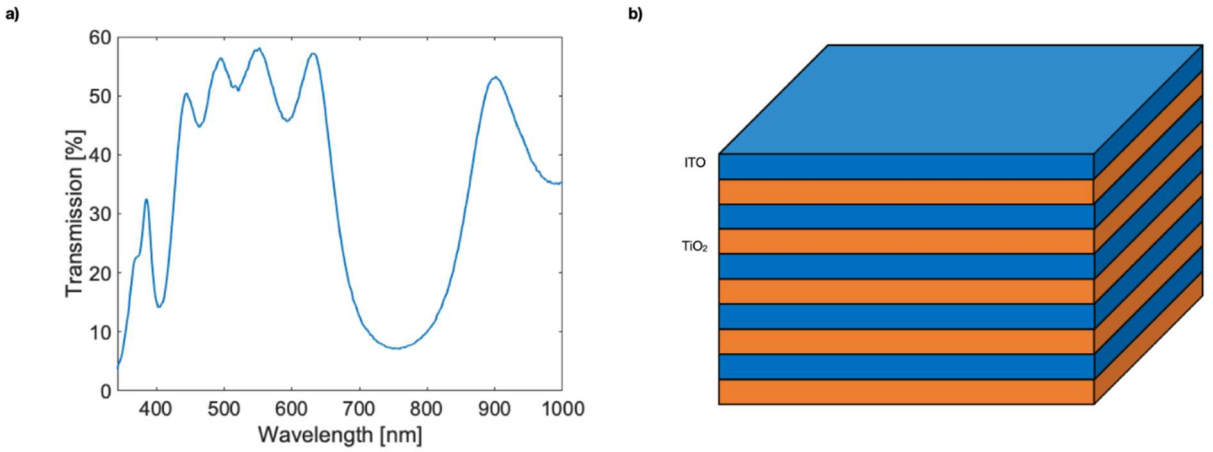

Figure 1 a) Steady-state transmission spectrum of the ITO/TiO_2 PC. b) Sketch of the one-dimensional multilayer PC.

We want to study how the transmission through the PC change upon photoexcitation of the plasmon. To do so we tune our OPA at 1550 nm where we have the ITO plasmonic absorption.
After the excitation of the plasmon in a timescale of about 10 fs due to electron scattering we have the plasmon dephasing and the creation of a non-thermalized Fermi distribution (FD). After this, within 100 fs an equilibrium hot FD is be created by electron-electron scattering. With our time resolution of about 100 fs we cannot see those events, but we can follow the subsequent relaxation of the hot-FD through electron-phonon scattering, that, happens in a timescale of less than 1 ps [29]. Finally, a much slower process take place which is the phonon-phonon scattering to get rid of the heat of the lattice.

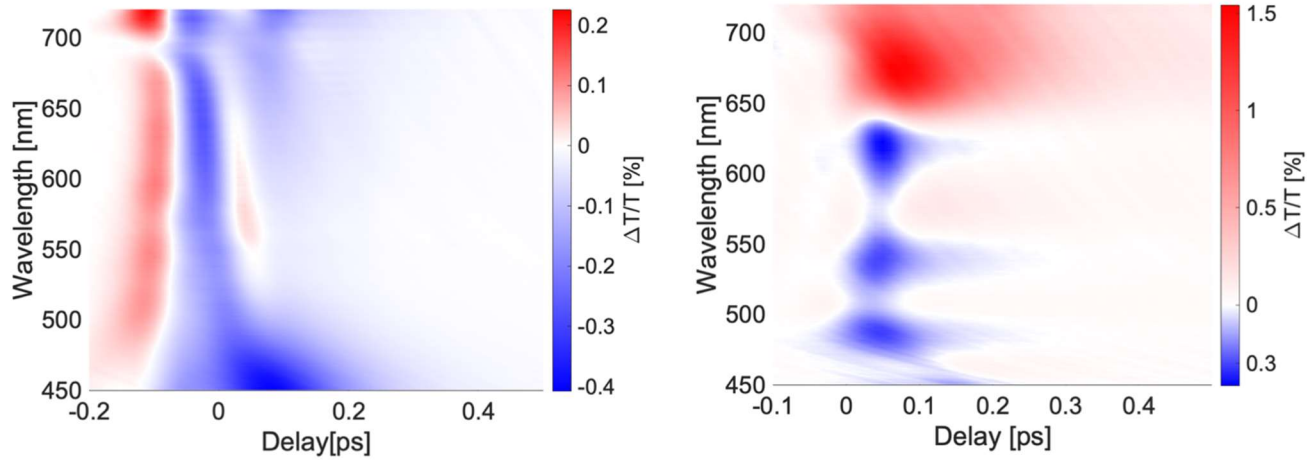

Figure 2 a) Transient response of ITO. b) Transient response of the PC

In Figure 2a we can see the transient response of the ITO layer. Around zero time delay we have the so-called cross phase modulation artifact (XPM), a coherent artifact that originates from the redistribution of the spectral component of the probe induced by the Kerr effect, a change in the refractive index caused by the strong pump pulse [30,31]. This fast change in the refractive index that is present only when pump and probe overlap in time on the glass substrate and is responsible for the initial positive-negative-positive signal [32], due to the fact that we don't have any exchange of energy between the glass substrate and the pump pulse, as soon as the two pulses are not overlapped in time anymore the artifact disappear and we don't have any contribution to the following dynamics. As we discussed above the relaxation dynamics are faster

than 1 ps and can be seen in Figure 2a. For bare ITO, after the XPM we have a negative signal at every wavelength in the visible region, by exciting the plasmon and creating the hot FD we are changing the dielectric function of the material, by changing both the plasmon resonance and the refractive index [33,24]. The plasmonic resonance depends on the effective mass of the carriers, ITO is a non-parabolic material, meaning that when we create a hot-FD the effective mass of the electrons changes by changing the position on the dispersion band, and so the plasma frequency does. A second effect is the change of the ϵ_∞ as it was modeled by Blemker et al [24], the epsilon inf change as a function of the electronic temperature of the Fermi Dirac distribution, a change of it will reflect in a change of the overall refractive index.

This leads to an ultrafast increase in the reflectivity of the ITO layer, and this is seen as a negative signal in terms of $\Delta T/T$ because more photons are reflected at the air-ITO interface.
This negative signal increase toward shorter wavelength, when we are around 440 nm we have a strong negative signal induced by the so-called inverse Moss-Burstein effect: before excitation all the transition from the intragap state and the conduction band are neglected because the levels are already filled with electrons, while when we create the hot-FD we free some space and those transition are now allowed resulting in a less transmitted probe.
In Figure 2b we can see the response of the PC, now we can see a different response that has positive and negative features. As we discussed above, this effect is induced by the change in the refractive index of the ITO. This modulation is still faster than 1 ps because it arises from the plasmon decay, by changing its refractive index the effective refractive index of the PC changes over time and so the PBG does, this shift can create complex modulation in the visible range, and a small ultrafast color shift is achieved.

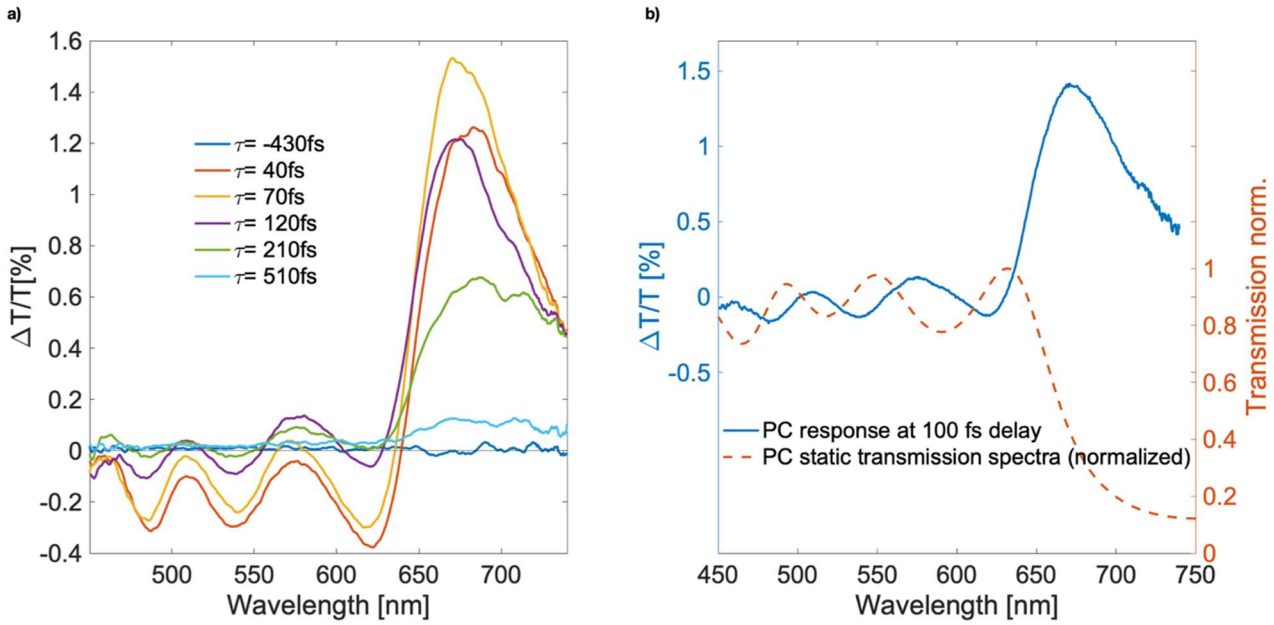

Figure 3 a) Spectra at fixed time delay of the PC. b) Static spectra and differential transmittivity signal of the PC.

In Figure 3a we can better appreciate the evolution of the spectral response at various fixed delay time, at around 510 fs the modulation has subsided. In Figure 3b we depicted the modulation at 100 fs delay and the static transmission spectra of the PC, here we can better appreciate the shift of the PBG, hence we can see the change of all the peaks and the "color" of the structure.

By changing the thickness, refractive index and the number of layers of the PC we can change the complexity and position of the resonance in the photonic bandgap. With this system we can modulate a visible beam by using an infrared pulse and the complexity of the modulation can be tuned accordingly. The de-excitation of the plasmon is faster than 1 ps, this gives us the capability to modulate an incoming visible beam with a repetition rate faster than 1 THz.

Conclusion

We fabricated a PC as a multilayer of ITO and TiO2, by designing the thickness and the number layers, we can create a pattern of destructive interference in the visible spectra that result in a modulated transmission. The differential transmission measurements show relaxation dynamics faster than 1 ps. The change in the refractive index of ITO upon photoexcitation of the plasmon resonance can used to create a PC that change its photonic bandgap in an ultrafast time scale and so to change its "color". This allow us to achieve all optical modulation in the visible region that can be tuned by designing the physical parameter of the PC accordingly.

Acknowledgement

This project has received funding from the European Research Council (ERC) under the European Union's Horizon 2020 research and innovation programme (grant agreement No. [816313]). This work has been supported by Fondazione Cariplo, grant n° 2018-0979.

References

[1] S. John, Strong localization of photons in certain disordered dielectric superlattices, Phys. Rev. Lett. 58 (1987) 2486–2489. https://doi.org/10.1103/PhysRevLett.58.2486.

[2] E. Yablonovitch, Inhibited Spontaneous Emission in Solid-State Physics and Electronics, Phys. Rev. Lett. 58 (1987) 2059–2062. https://doi.org/10.1103/PhysRevLett.58.2059.

[3] J.D. Joannopoulos, ed., Photonic crystals: molding the flow of light, 2nd ed, Princeton University Press, Princeton, 2008.

[4] K. Sakoda, Optical Properties of Photonic Crystals, 2nd ed., Springer-Verlag, Berlin Heidelberg, 2005. https://doi.org/10.1007/b138376.

[5] T. Komikado, S. Yoshida, S. Umegaki, Surface-emitting distributed-feedback dye laser of a polymeric multilayer fabricated by spin coating, Appl. Phys. Lett. 89 (2006) 061123. https://doi.org/10.1063/1.2336740.

[6] F. Scotognella, A. Monguzzi, M. Cucini, F. Meinardi, D. Comoretto, R. Tubino, One Dimensional Polymeric Organic Photonic Crystals for DFB Lasers, International Journal of Photoenergy. (2008). https://doi.org/10.1155/2008/389034.

[7] F. Scotognella, A. Monguzzi, F. Meinardi, R. Tubino, DFB laser action in a flexible fully plastic multilayer, Phys. Chem. Chem. Phys. 12 (2009) 337–340. https://doi.org/10.1039/B917630F.

[8] F. Scotognella, D.P. Puzzo, M. Zavelani-Rossi, J. Clark, M. Sebastian, G.A. Ozin, G. Lanzani, Two-Photon Poly(phenylenevinylene) DFB Laser, Chem. Mater. 23 (2011) 805–809. https://doi.org/10.1021/cm102102w.

[9] R. Li Voti, Optimization of a perfect absorber multilayer structure by genetic algorithms, J. Eur. Opt. Soc.-Rapid Publ. 14 (2018) 1–12. https://doi.org/10.1186/s41476-018-0079-7.

[10] Y. Li, Z. Liu, H. Zhang, P. Tang, B. Wu, G. Liu, Ultra-broadband perfect absorber utilizing refractory materials in metal-insulator composite multilayer stacks, Opt. Express, OE. 27 (2019) 11809–11818. https://doi.org/10.1364/OE.27.011809.

[11] S.Y. Choi, M. Mamak, G. von Freymann, N. Chopra, G.A. Ozin, Mesoporous Bragg Stack Color Tunable Sensors, Nano Lett. 6 (2006) 2456–2461. https://doi.org/10.1021/nl061580m.

[12] A. von Mankowski, K. Szendrei-Temesi, C. Koschnick, B.V. Lotsch, Improving analyte selectivity by post-assembly modification of metal–organic framework based photonic crystal sensors, Nanoscale Horiz. 3 (2018) 383–390. https://doi.org/10.1039/C7NH00209B.
[13] V. González-Pedro, M.E. Calvo, H. Míguez, Á. Maquieira, Nanoparticle Bragg reflectors: A smart analytical tool for biosensing, Biosensors and Bioelectronics: X. 1 (2019) 100012. https://doi.org/10.1016/j.biosx.2019.100012.
[14] H. Megahd, C. Oldani, S. Radice, A. Lanfranchi, M. Patrini, P. Lova, D. Comoretto, Aquivion–Poly(N-vinylcarbazole) Holistic Flory–Huggins Photonic Vapor Sensors, Advanced Optical Materials. 9 (2021) 2002006. https://doi.org/10.1002/adom.202002006.
[15] H. Megahd, P. Lova, D. Comoretto, Universal Design Rules for Flory–Huggins Polymer Photonic Vapor Sensors, Advanced Functional Materials. 31 (2021) 2009626. https://doi.org/10.1002/adfm.202009626.
[16] C. López, Materials Aspects of Photonic Crystals, Adv. Mater. 15 (2003) 1679–1704. https://doi.org/10.1002/adma.200300386.
[17] Z.V. Vardeny, A. Nahata, A. Agrawal, Optics of photonic quasicrystals, Nature Photonics. 7 (2013) 177–187. https://doi.org/10.1038/nphoton.2012.343.
[18] D.S. Wiersma, Disordered photonics, Nature Photonics. 7 (2013) 188–196. https://doi.org/10.1038/nphoton.2013.29.
[19] A. Chiasera, F. Scotognella, L. Criante, S. Varas, G.D. Valle, R. Ramponi, M. Ferrari, Disorder in Photonic Structures Induced by Random Layer Thickness, Sci Adv Mater. 7 (2015) 1207–1212. https://doi.org/10.1166/sam.2015.2249.
[20] E. Feigenbaum, K. Diest, H.A. Atwater, Unity-Order Index Change in Transparent Conducting Oxides at Visible Frequencies, Nano Lett. 10 (2010) 2111–2116. https://doi.org/10.1021/nl1006307.
[21] S. Heo, A. Agrawal, D.J. Milliron, Wide Dynamic Range in Tunable Electrochromic Bragg Stacks from Doped Semiconductor Nanocrystals, Advanced Functional Materials. 29 (2019) 1904555. https://doi.org/10.1002/adfm.201904555.
[22] L. Moscardi, G.M. Paternò, A. Chiasera, R. Sorrentino, F. Marangi, I. Kriegel, G. Lanzani, F. Scotognella, Electro-responsivity in electrolyte-free and solution processed Bragg stacks, J. Mater. Chem. C. (2020). https://doi.org/10.1039/D0TC02437F.
[23] G. Cerullo, C. Manzoni, L. Lüer, D. Polli, Time-resolved methods in biophysics. 4. Broadband pump–probe spectroscopy system with sub-20 fs temporal resolution for the study of energy transfer processes in photosynthesis, Photochem. Photobiol. Sci. 6 (2007) 135–144. https://doi.org/10.1039/B606949E.
[24] M.A. Blemker, S.L. Gibbs, E.K. Raulerson, D.J. Milliron, S.T. Roberts, Modulation of the Visible Absorption and Reflection Profiles of ITO Nanocrystal Thin Films by Plasmon Excitation, ACS Photonics. 7 (2020) 1188–1196. https://doi.org/10.1021/acsphotonics.9b01825.
[25] A.J. Haider, Z.N. Jameel, I.H.M. Al-Hussaini, Review on: Titanium Dioxide Applications, Energy Procedia. 157 (2019) 17–29. https://doi.org/10.1016/j.egypro.2018.11.159.
[26] M. Born, E. Wolf, A.B. Bhatia, P.C. Clemmow, D. Gabor, A.R. Stokes, A.M. Taylor, P.A. Wayman, W.L. Wilcock, Principles of Optics: Electromagnetic Theory of Propagation, Interference and Diffraction of Light, 7th ed., Cambridge University Press, 1999. https://doi.org/10.1017/CBO9781139644181.
[27] F. Scotognella, A. Chiasera, L. Criante, E. Aluicio-Sarduy, S. Varas, S. Pelli, A. Łukowiak, G.C. Righini, R. Ramponi, M. Ferrari, Metal oxide one dimensional photonic crystals made by RF sputtering and spin coating, Ceramics International. 41 (2015) 8655–8659. https://doi.org/10.1016/j.ceramint.2015.03.077.

[28] I. Kriegel, F. Scotognella, L. Manna, Plasmonic doped semiconductor nanocrystals: Properties, fabrication, applications and perspectives, Physics Reports. 674 (2017) 1–52. https://doi.org/10.1016/j.physrep.2017.01.003.
[29] M.Z. Alam, I. De Leon, R.W. Boyd, Large optical nonlinearity of indium tin oxide in its epsilon-near-zero region, Science. 352 (2016) 795–797. https://doi.org/10.1126/science.aae0330.
[30] M. Lorenc, M. Ziolek, R. Naskrecki, J. Karolczak, J. Kubicki, A. Maciejewski, Artifacts in femtosecond transient absorption spectroscopy, Applied Physics B: Lasers and Optics. 74 (2002) 19–27. https://doi.org/10.1007/s003400100750.
[31] K. Ekvall, P. van der Meulen, C. Dhollande, L.-E. Berg, S. Pommeret, R. Naskrecki, J.-C. Mialocq, Cross phase modulation artifact in liquid phase transient absorption spectroscopy, Journal of Applied Physics. 87 (2000) 2340–2352. https://doi.org/10.1063/1.372185.
[32] A. Bresci, M. Guizzardi, C.M. Valensise, F. Marangi, F. Scotognella, G. Cerullo, D. Polli, Removal of cross-phase modulation artifacts in ultrafast pump–probe dynamics by deep learning, APL Photonics. 6 (2021) 076104. https://doi.org/10.1063/5.0057404.
[33] R.W. Johns, M.A. Blemker, M.S. Azzaro, S. Heo, E.L. Runnerstrom, D.J. Milliron, S.T. Roberts, Charge carrier concentration dependence of ultrafast plasmonic relaxation in conducting metal oxide nanocrystals, J. Mater. Chem. C. 5 (2017) 5757–5763. https://doi.org/10.1039/C7TC00600D.